DNA charge neutralization by linear polymers. II. Reversible binding

E. Maltsev, J. A. D. Wattis,* and H. M. Byrne†
Centre for Mathematical Medicine, School of Mathematical Sciences, University Park, University of Nottingham, Nottingham, NG7 2RD, United Kingdom

(Received 5 January 2006; revised manuscript received 9 August 2006; published 27 October 2006)

We model the way in which polymers bind to DNA and neutralize its charged backbone by analyzing the dynamics of the distribution of gaps along the DNA. We generalize existing theory for irreversible binding to construct deterministic models which include polymer removal, movement along the DNA, and allow for binding with overlaps. We show that reversible binding alters the capacity of the DNA for polymers by allowing the rearrangement of polymer positions over a longer time scale than when binding is irreversible. When the polymers do not overlap, allowing reversible binding increases the number of polymers adhered and hence the charge that the DNA can accommodate; in contrast, when overlaps occur, reversible binding reduces the amount of charge neutralized by the polymers.

DOI: 10.1103/PhysRevE.74.041918 PACS number(s): 82.20.−w, 82.30.−b, 82.39.−k

I. INTRODUCTION

In this paper we extend a deterministic mathematical model of polymer binding [1] to include removal and movement of polymers along the DNA plasmid. Both the kinetics of reversible binding and the steady state (equilibrium) solutions are studied. The DNA is modeled as a single one-dimensional strand, with uniformly spaced binding sites. The model is used to analyze how the distribution of gap sizes evolves when polymers attach to the DNA. Such knowledge allows us to calculate the fraction of DNA sites occupied by the polymers and the resulting charge neutralization.

The resulting model has the form of a generalized "parking problem," also known as "random sequential absorption" (RSA) and has been studied by Rényi [2] and Bonnier *et al.* [3]. Epstein [4,5] has applied the RSA model to polymer absorption, where it is referred to as "the excluded site binding model" and has been used to estimate the time variation of charge neutralization, as well as the equilibrium value [6]. One area where knowledge of charge neutralizations is vital is in the delivery of gene therapy. The successful introduction of DNA into the nucleus of an abnormal cell requires the DNA to be compacted: one way of achieving this is through the use of cationic polymers [7].

A recent review of RSA models is given by Talbot *et al.* [8]. While this describes the generalization of RSA to the adsorbtion of particles with a variety of shapes and a range of sizes to a surface, the problem of reversible binding is only briefly addressed. Exact solutions and large-time asymptotic results of RSA systems have been derived by Ben-Naim and Krapivsky [9], who also consider generalized RSA models which include reversible binding (Krapivsky and Ben-Naim [10]). Both Brewer *et al.* [11,12] and Lever *et al.* [13] show that DNA condensation by polymers is a reversible process. Tarjus *et al.* [14] analyzes a generalized RSA model in which either binding and desorption or binding and surface diffusion of polymer on DNA occurs. Although complex, the model is analyzed theoretically in the low coverage limit. This contrasts with our results for an alternative generalized RSA model with reversible binding and surface diffusion of adsorbed polymers, where asymptotic results are obtained for the high coverage regime. Other extensions of RSA to include cooperative effects have been studied by Evans [15] and Barma [16]; the latter including diffusion of adsorbed particles along the substrate. Van Tassel *et al.* [17] also present a generalized model of partially reversible RSA. In the spirit of Michaelis-Menten reaction kinetics, they assume that upon binding to a substrate, the polymer which is in its native state and the substrate form a metastable complex. It is possible for this complex to unbind or for the polymer to undergo some conformational change in which it becomes irreversibly bound to the substrate. They argue that such a model is more accurate than Langmuir-models due to the treatment of surface blocking.

Teif [18] models polymer adsorption to DNA with different on and off rates for normal and condensed DNA and incorporates the effect of dissolved salt on the condensation process. His models explain decondensation of the DNA at very high polymer concentrations through resolubilization of the DNA. The cooperativity parameter in the McGhee–von Hippel model can be motivated by the fact that some polymers have sticky ends and free polymer is more likely to bind adjacent to an already-bound polymer than in the interior of a gap. However, many condensing polymers do not have sticky ends yet still exhibit a cooperative binding effect, so an alternative justification is required. Brewer *et al.* [11] shows that for DNA condensation into toroids by adsorption of protamine, polymer adhesion is the rate-limiting step in condensation. If condensation occurs immediately upon polymer binding, then the DNA will locally change its shape at and near the region of bound polymers; this provides a mechanism for the rates of polymer attachment and removal to differ near already bound polymers from those in uncondensed DNA.

The remainder of this section contains an introduction to the notation we use to derive our models of polymer adherence to DNA, and a summary of the results obtained in Ref. [1] for irreversible binding with and without overlaps. In

*Corresponding author. Electronic address: Jonathan.Wattis@nottingham.ac.uk
†Electronic address: Helen.Byrne@nottingham.ac.uk

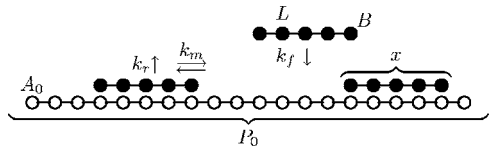

FIG. 1. Summary of polymer binding notation for a case when $A_0=1$, $P_0=20$, $x=5$, $L_0=3$, $L=1$, and $B=2$.

Sec. I A we summarize the modeling approach and quote the model for irreversible binding, the gap distribution kinetics for reversible binding are derived in Sec. II. A corresponding model for partially overlapping polymers is derived in Sec. III; this model allows charge inversion [19]. This occurs when so much polymer adheres to the DNA that the complex acquires a positive charge. The model is extended to include polymer motion along the DNA in Sec. IV. Even though the dynamic model is slow to solve numerically when motion is included, the asymptotic solutions for fast motion allow us to calculate the charge neutralization associated with polymer binding with or without motion (see Sec. IV B) and our asymptotic solution method is applied to find steady state solutions in Sec. IV C. Reversible binding of overlapping polymers with motion is studied in Sec. V. The results are discussed in Sec. VI.

A. Modeling approach

Here, we follow the modeling approach introduced in Ref. [1]. We define x to be the length of the polymer, and p to be the length of the gap in which the incoming polymer will bind. Both x and p are integers, and for the case of charged polymers binding to DNA they represent numbers of base pairs. We define $N_p(t)$ to be the number of gaps of length p at time t. In the simpler cases only positive gap lengths are considered, however, we show later that binding with overlaps can be incorporated into such models by treating overlaps as gaps with negative lengths.

The length of the DNA molecule is P_0 (each site corresponds to a negatively charged phosphate group) and the concentration of the DNA is measured in moles (M) and denoted by A_0. The following parameters (with corresponding units) are used: binding, removal, and movement rates k_f ($s^{-1}\,M^{-1}$), k_r (s^{-1}), and k_m (sites $\times$ s^{-1}), respectively. The concentrations of bound and free polymers in solution are B (M) and L (M), respectively. L_0 (M) denotes the initial number of polymers in solution (so $B=L_0-L$). The notation for the length, rates and concentrations is summarized in Fig. 1.

As polymers adhere, they neutralize the negative charge of the DNA; however, we ignore the electrostatic-thermodynamic properties of the system in favor of a model which is more faithful to the geometric constraints of binding and blocking of binding sites. Our model is thus more closely related to models of random sequential adsorption rather than the counterion condensation theories of Manning [20] and Rouzina and Bloomfield [21]. Two physical quantities derived from the gap size distribution can be used to calculate the extent of charge neutralization. They are the total number of gaps M_0 as defined by

$$M_0(t) = \sum_{p=0}^{P_0} N_p(t) \tag{1}$$

and the total length of gaps M_1,

$$M_1(t) = \sum_{p=1}^{P_0} pN_p(t). \tag{2}$$

The charge neutralization θ is defined to be the proportion of charges on the DNA neutralized by the polymer. This can be calculated in two ways

$$\theta(t) = \frac{x[M_0(t)-1]}{P_0} = \frac{P_0 - M_1(t)}{P_0}, \tag{3}$$

since M_0-1 is the number of polymer molecules attached to the DNA plasmid and P_0-M_1 is the total number of sites occupied by the polymers. Thus the identity

$$xM_0(t) + M_1(t) = P_0 + x, \tag{4}$$

is valid for all t.

Since the number of polymers bound to the DNA is M_0-1, the concentration of bound polymers is $B=A_0(M_0-1)$, where A_0 is the molar concentration of DNA. Hence the molar concentration of free polymers $L(t)$ can be expressed in terms of the sum of all gaps as

$$L(t) = L_0 - B(t) = L_0 - A_0[M_0(t)-1], \tag{5}$$

where $L_0=L(t=0)$ is the molar concentration of polymers in the solution before any binding occurs.

The rate at which the gap distribution N_p evolves over time is calculated by considering the rates at which gaps are created and destroyed during polymer adhesion (F_p), removal (U_p), and movement (V_p) of polymers. Combining the above rates results in

$$\frac{dN_p}{dt} = F_p^f - F_p^r + U_p^f - U_p^r + V_p^f - V_p^r, \tag{6}$$

where f and r in the superscripts refer to the rates at which gaps are formed and removed, respectively.

B. Irreversible binding

Irreversible binding without motion occurs when F_p^f and F_p^r are the only nonzero terms in Eq. (6). When the irreversible binding terms [1,22] are separated into gap creation and removal components we have

$$F_p^f = 2K_f \sum_{g=p+x}^{P_0} N_g, \tag{7a}$$

$$F_p^r = K_f(p-x+1)N_p, \tag{7b}$$

where K_f is the binding rate defined by $K_f=k_fL(t)$, and k_f is a rate constant. The full system of equations for the gap distribution kinetics is

$$\frac{dN_p}{dt} = -F_p^r \quad (P_0-x+1 \le p \le P_0), \tag{8a}$$

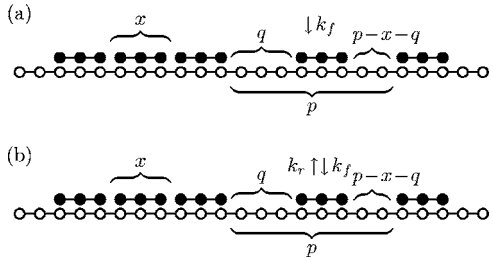

FIG. 2. (a) Illustration of how polymer adhesion destroys a gap of size p and leads to the formation of gaps of length q and $p-x-q$. (b) Illustration of how polymer removal can lead to the formation of a gap of length p, and how polymer adhesion leads to the formation of a gap of length q.

$$\frac{dN_p}{dt} = F_p^f - F_p^r \quad (x \le p \le P_0 - x), \tag{8b}$$

$$\frac{dN_p}{dt} = F_p^f \quad (0 \le p \le x - 1). \tag{8c}$$

See Fig. 2(a) for an illustration of gaps formed as polymers bind without overlaps. In Ref. [1] the system of equations (8) was solved numerically for a variety of cases. Figure 5 shows how the charge neutralization $\theta(t)$ defined in Eq. (3) evolves over time (dashed line). Recurrence relations for the steady-state value of θ are derived, and an asymptotic analysis enables approximate solutions to be constructed. The curve does not asymptote to $\theta=1$ because the polymers have length $x>1$, they bind at random positions, and as a result gaps form between bound polymers. When all gaps are smaller than x, no further binding can occur, yet not all of the charges on the DNA have been neutralized. Thus the final charge neutralization will be below 100%. Guided by experimental work involving long polymers and longer strands of DNA [23], the particular scalings considered are $x \gg 1$ and $P_0=\mathcal{O}(x^2)$, and in this limit we obtain

$$\theta \sim \frac{3x}{4x-1}\left(1 - \frac{x-1}{3P_0}\right).$$

In Sec. II, we generalize Eq. (8) to allow for polymer removal and polymer motion along the DNA.

The case of irreversible binding with overlaps is also considered in Ref. [1]; here the gap creation and removal components are

$$F_p^f = 2K_f \sum_{g=p+1}^{P_0} N_g, \tag{9a}$$

$$F_p^{f-} = 2K_f \sum_{g=1}^{P_0} N_g, \tag{9b}$$

$$F_p^r = K_f(p + x - 1)N_p, \tag{9c}$$

where K_f is the binding rate defined by $K_f=k_fL(t)$, and k_f is a rate constant. Gaps with $p<0$ describe overlaps of size $-p$, and the new term F_p^{f-} denotes the rate of creation of overlaps.

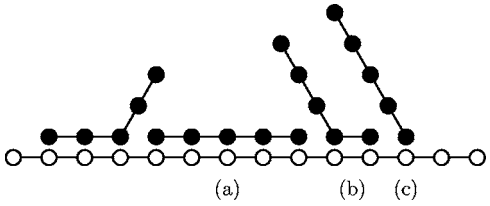

FIG. 3. Polymers of length $x=5$ with overlaps.

The full system of equations for the gap distribution kinetics is

$$\frac{dN_{P_0}}{dt} = -F_{P_0}^r, \tag{10a}$$

$$\frac{dN_p}{dt} = F_p^f - F_p^r \quad (1 \le p \le P_0 - 1), \tag{10b}$$

$$\frac{dN_p}{dt} = F_p^{f-} \quad (1 - x \le p \le 0). \tag{10c}$$

In place of Eqs. (1) and (2) we now have

$$M_0 = \sum_{p=1-x}^{P_0} N_p(t), \quad M_1 = \sum_{p=1-x}^{P_0} pN_p(t); \tag{11}$$

with these definitions, the identity (4) and formula (3) both still hold.

See Fig. 3 for an illustration of polymer binding with overlaps. In Sec. III (10) is generalized to include polymer motion and removal. Our earlier paper [1] presents the results of numerical simulations of irreversible binding models, together with asymptotic analysis of the system for long DNA plasmids and long polymers. Plots of charge neutralization over time have the same sigmoidal shape as the dashed line in Fig. 5, although they rise to values between $\theta=1$ and $\theta=3$ (see, for example, the solid line in Fig. 10). For $x \sim \sqrt{P_0} \gg 1$ asymptotic analysis of the charge neutralization recurrence relation showed that $\theta \sim 2-2/x+x/P_0$. It was also found that at equilibrium, the distribution of overlap sizes is uniform, in contrast with the equilibrium distribution of gap sizes in the nonoverlapping case where there are many more smaller gaps.

II. NONOVERLAPPING REVERSIBLE BINDING

In this section we extend the model of nonoverlapped binding (8) to incorporate reversible binding, so that in Eq. (6), $F_p^{f,r}$ and $U_p^{f,r}$ are nonzero but $V_p^{f,r}=0$. The model is derived in Sec. II A and numerical results are presented in Sec. II B.

A. Kinetics of gap creation and destruction due to polymer unbinding

A gap of size p is created when a polymer of length x is removed if two gaps of length q and $p-q-x$ are destroyed [see Fig. 2(b)]: we represent this situation as follows:

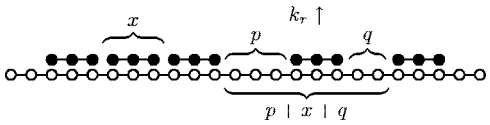

FIG. 4. Illustration of the destruction of a p gap due to polymer unbinding.

$$(p-x-q)+(q)\rightarrow(p). \tag{12}$$

The frequency at which the shorter gaps occur is proportional to N_qN_{p-q-x}. These two gaps have to be separated by a bound polymer. Since the gap N_{p-q-x} could be located in any of M_0 positions, the frequency at which both gaps occur separated by just one bound polymer is

$$\frac{N_qN_{p-q-x}}{M_0}. \tag{13}$$

If the polymers are removed from the DNA at the rate k_r (s^{-1}) then the total number of gaps of length p that are created when Eq. (12) occurs is

$$U_p^f=\frac{k_r}{M_0}\sum_{q=0}^{p-x}N_qN_{p-x-q}. \tag{14}$$

With U_p^f defined by Eq. (14) we use a similar argument to determine how gaps of length p are destroyed when a polymer is removed from the DNA, and hence specify U_p^r.

A gap of length p will be destroyed by removal if there is a corresponding gap of length q separated by one bound polymer of length x. In this case, the two gaps (p,q) coalesce to form one larger gap of length $p+x+q$ (see Fig. 4):

$$(p)+(q)\rightarrow(p+x+q). \tag{15}$$

Adopting the same approach that was used to obtain Eq. (14), but noting that two gaps are destroyed whenever a polymer unbinds, we deduce that the rate of gap removal due to polymer unbinding U_p^r is given by

$$U_p^r=\frac{2k_r}{M_0}N_p\sum_{q=0}^{P_0-p-x}N_q. \tag{16}$$

When $P_0\gg x$, Eq. (16) can be approximated by

$$U_p^r=2k_rN_p. \tag{17}$$

The gap creation (14) and destruction (16) terms are combined with Eq. (8) to obtain the following differential equations for the kinetics of gap distribution of the nonoverlapping reversible binding system

$$\frac{dN_p}{dt}=-F_p^r+U_p^f \quad (P_0-x+1\le p\le P_0), \tag{18a}$$

$$\frac{dN_p}{dt}=F_p^f-F_p^r+U_p^f-U_p^r \quad (x\le p\le P_0-x), \tag{18b}$$

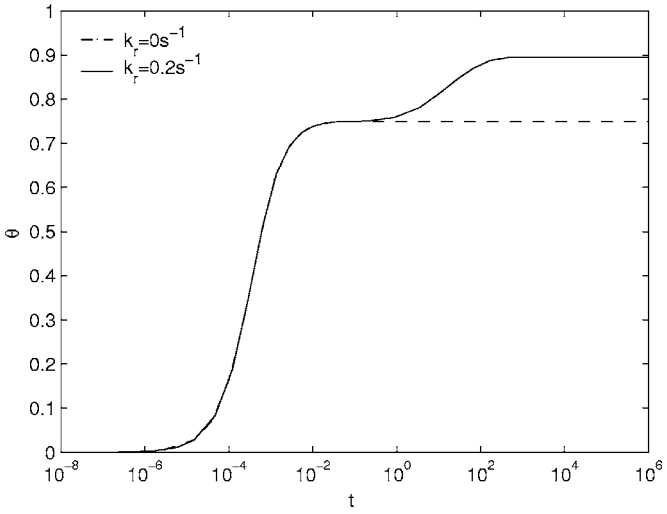

FIG. 5. Curves showing how, for nonoverlapped binding, polymer removal affects the charge neutralization dynamics $\theta(t)$ and, in particular, increases the equilibrium charge neutralization. Parameter values $L_0=10^{-6}$ M, $A_0=2\times10^{-9}$ M, $P_0=500$ sites, $x=20$ sites, $k_f=10^8$ M^{-1} s^{-1}.

$$\frac{dN_p}{dt}=F_p^f-U_p^r \quad (0\le p\le x-1). \tag{18c}$$

We note that gaps of size $P_0-x+1\le p\le P_0$ cannot be destroyed by polymer removal and therefore Eq. (18a) contains only the gap creation term U_p^f. When polymers leave the DNA, they always create gaps at least as long as the polymer itself. Hence when considering short gaps with $0\le p\le x-1$ only gap destruction terms (U_p^r) are present [see Eq. (18c)].

B. Numerical solution

The evolution of gap distributions $N_p(t)$ was calculated by solving equations (18) numerically using a semiexplicit interpolation method [24] with adaptive step-size control written and compiled using FORTRAN 90. The charge neutralization was calculated from $\theta=x(M_0-1)/P_0$, where M_0 is the total number of gaps [see Eq. (3)].

When the polymers bind reversibly to the DNA we find a second phase of kinetic behavior which occurs over a longer time scale, during which the charge neutralization exceeds that for irreversible binding (see Figs. 5, 7, and 8). The initial rise in charge neutralization is the same for reversible and irreversible binding. That the inclusion of polymer removal causes a later *increase* in charge neutralization is perhaps counterintuitive. During this latter phase of the process, polymer desorption allows the rearrangement of polymers on the DNA: polymer removal and reattachment leads to changes in the distribution of gaps sizes. The equilibrium gap distribution corresponding to the charge neutralization curves shown in Fig. 5 is plotted in Fig. 6 and shows that reversible binding results in a less uniform distribution of gap sizes at equilibrium than is the case with irreversible binding. Over the longer time scale, polymer rearrangement causes an increased frequency of shorter gaps, creating other gaps large

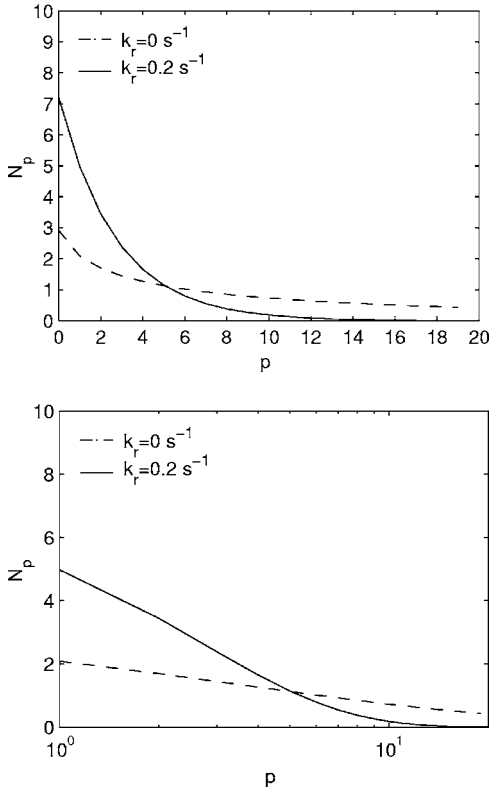

FIG. 6. Curves showing how, for nonoverlapped binding, polymer removal changes the equilibrium gap distribution. Parameter values are as in Fig. 5.

enough for extra polymer landing and hence is consistent with the increased charge neutralization observed in Fig. 5.

1. Effect of varying the kinetic rates

The plot in Fig. 7 shows the effect on charge neutralization of varying the binding and removal rates. The first effect

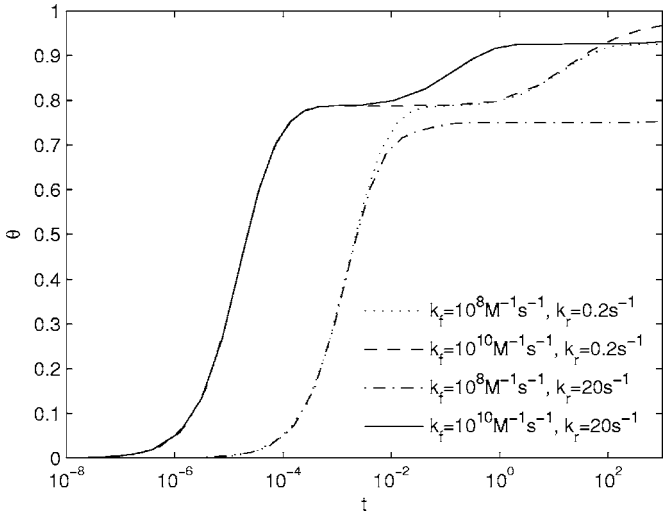

FIG. 7. Series of curves showing how changing the binding and removal rates influences the charge neutralization dynamics $\theta(t)$. Parameter values $L_0=10^{-6}$ M, $A_0=5\times10^{-9}$ M, $P_0=200$ sites, $x=5$ sites.

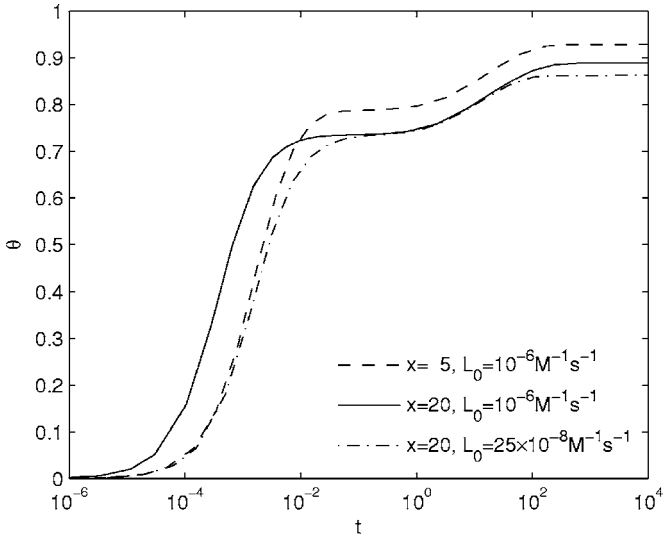

FIG. 8. Series of curves illustrating how the length of the polymer, with adjusted binding rate, affects the charge neutralization dynamics $\theta(t)$. Parameter values $A_0=5\times10^{-9}$ M, $P_0=200$ sites, $k_f=10^8$ M^{-1} s^{-1}, $k_r=0.2$ s^{-1}.

to notice is that the time of the initial rise from $\theta=0$ depends on the rate of binding k_f, the solid and dashed curves are initially coincident ($k_f=10^{10}$ M^{-1} s^{-1}), as are the dotted and the dash-dotted lines ($k_f=10^8$ M^{-1} s^{-1}). For the parameter values used, the simulations show that the rate of removal does not influence the binding kinetics until θ exceeds one half. (By making the removal rate k_r extremely large, it is possible to make the equilibrium charge neutralization curve asymptote to a low value of θ.)

If $k_r=0$ the initial plateau is maintained for all subsequent times, however, if $k_r>0$, there is a second phase of kinetics occurring over a longer time scale, in which higher charge neutralizations are accessible as a second plateau in θ is attained. In the case of the dash-dotted line, the removal rate is so large that only one plateau is seen. The height of the final plateau depends on the ratio of the removal and binding rates, thus the dotted curve and the solid curve approach the same limit, with the dotted curve simply being shifted in the horizontal direction, since its rates are simply multiples of those for the solid curve.

When the removal rate is increased, with the binding rate fixed the equilibrium charge neutralization falls (compare dotted with dash-dotted line). We note also that when only the binding rate is increased and the removal rate fixed then the initial increase in θ occurs earlier and the final equilibrium value of θ is also increased (compare dashed and dotted lines).

2. Effect of varying the polymer length

The effect of changing polymer length on charge neutralization is shown in Fig. 8. We find that initially longer polymers adhere at a greater rate, leading to faster kinetics, but that the equilibrium charge neutralization is lower (compare solid and dashed curves in Fig. 8).

There are two phenomena that our model has not yet taken into account. First, since longer polymers have greater

charge, their binding and removal rates may differ from those of shorter polymers. Secondly, the initial concentration of polymers was identical in both cases. Therefore in the case of longer polymers, there are more polymeric charges available to neutralize the DNA. Fewer longer polymers are required to cover the DNA surface and hence the reduction in the binding rate will be greater in the case of shorter polymers. One might expect this to promote higher charge neutralization when longer polymers are used. However, longer polymers also give rise to longer gaps on the DNA plasmid, reducing its charge neutralization. In practice, the latter effect prevails: thus in Fig. 8 the equilibrium value of θ is lower for the longer polymer (compare solid and dashed curves).

L_0x is the total amount of charge in the system. If we increase the polymer length (x) while holding L_0 fixed then this will increase the total amount of polymer charge available to neutralize the DNA. From Fig. 8 we note that a simple increase in x, with L_0 fixed, leads to accelerated kinetics, a lower intermediate plateau and a slightly lower equilibrium value of θ. We now investigate the effect of increasing the polymer length (x) and decreasing L_0 so that the total amount of polymer charge (xL_0) is held constant.

Comparing dashed and dot-dashed lines in Fig. 8 indicates that an increase in polymer length combined with a reduction in the binding rate (by a factor of 4 in both cases) results in an approach to the first plateau of the graph on a similar time scale. This corresponds to the equilibrium value of the charge-neutralization in the irreversible binding case, which is higher for short polymers. Following that, the kinetics of the dash-dotted curve ($x=20$, $L_0=0.25\times10^{-6}$ $M^{-1}s^{-1}$) are similar to those of the original, 20-site polymer (solid curve, $L_0=10^{-6}$) but the reversible binding equilibrium (second plateau) is lower for $L_0=0.25\times10^{-6}$ than for $L_0=10^{-6}$, indicating a more complex dependence on the polymer length, polymer concentration in the solution, and binding and removal rates.

III. OVERLAPPING REVERSIBLE BINDING

We now generalize the above model of reversible binding to include cases when polymers bind with only some of their charges, leaving ends which overlap with neighboring bound polymers. The effect can be incorporated into our models quite naturally by describing an overlap of p sites as a gap of size $-p$. This again corresponds to Eq. (6) with $F_p^{f,r}$ and $U_p^{f,r}$ nonzero and $V_p^{f,r}=0$.

A. Removal kinetics

Even when negative gap lengths are allowed, two gaps at the ends of a polymer are transformed into one larger gap when a polymer is removed from the DNA plasmid. The gap is always of positive length since the polymer had to be attached to the DNA with at least one monomer unit. The creation of gaps of size p due to removal is proportional to the total number of gaps of sizes q and $p-x-q$ with $1-x\leq q\leq P_0-1$. Thus we have a gap creation term which depends on the removal rate and applies to gaps that are at least one-site long, namely,

$$U_p^f=\frac{k_r}{M_0}\sum_{q=1-x}^{p-1}N_qN_{p-x-q}, \tag{19}$$

where k_r is the removal rate. The lower and upper limits correspond to the largest possible overlap.

When a gap of size p is destroyed by polymer removal, the removal rate is proportional to the number of such gaps; and since two gaps are destroyed when a polymer is removed, it is also dependent on the number and size of other gaps

$$U_p^r=2\frac{k_rN_p}{M_0}\sum_{q=1-x}^{P_0-p-x}N_q. \tag{20}$$

It is possible for overlaps to overlap; this depends on the order in which adjacent polymers attach to the DNA. An example of possible overlaps is illustrated in Fig. 3. Polymer (b) shares an overlap of length 3 with polymer (a) and an overlap of length 4 with polymer (c); polymer (c) overlaps (a) as well as (b).

Polymer removal is modeled in a way similar to that described in Sec. II. The only difference is that when polymers are allowed to overlap, the smallest gap possible has length $1-x$ (corresponding to an overlap of length $x-1$). In this case our governing equations for binding and removal are

$$\frac{dN_{P_0}}{dt}=-F_{P_0}^r+U_{P_0}^f, \tag{21a}$$

$$\frac{dN_p}{dt}=F_p^f-F_p^r+U_p^f-U_p^r\quad(1\leq p\leq P_0-1), \tag{21b}$$

$$\frac{dN_p}{dt}=F_p^{f-}+U_p^f-U_p^r\quad(2-x\leq p\leq 0), \tag{21c}$$

$$\frac{dN_{1-x}}{dt}=F_{1-x}^{f-}-U_{1-x}^r. \tag{21d}$$

B. Numerical results

As in Sec. II B, the overlapped binding equations were solved using a semi-implicit extrapolation method with adaptive step-size control. The charge neutralization for typical simulations are presented in Fig. 9.

The effect of polymer removal is very different when there is overlapped binding. Whereas the removal of polymers for nonoverlapped simulations resulted in *higher* steady-state charge neutralizations (see Figs. 7 and 8) in the overlapped case it results in a *lower* equilibrium charge neutralization (see Fig. 9).

We note from Fig. 9 that the equilibrium charge neutralization appears to depend only on the polymer length, and is independent of polymer concentration. This is in clear contrast to the system where overlaps are prohibited (Fig. 8), where charge-neutralization depends on a complex combina-

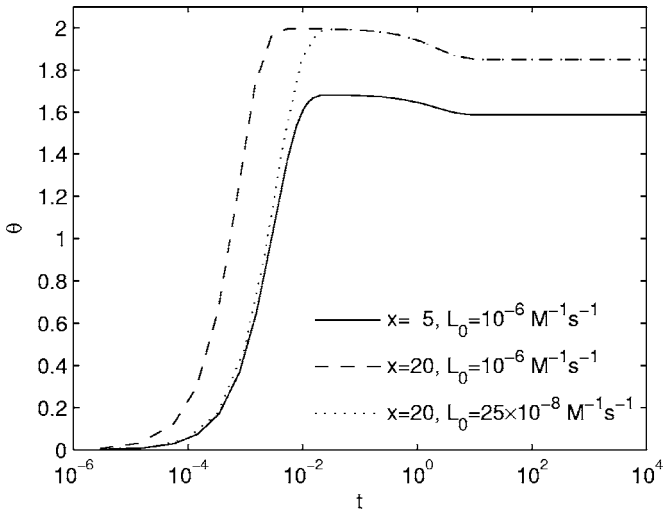

FIG. 9. Effect of polymer length on the kinetics of binding ($A_0=5\times10^{-9}$ M, $P_0=200$ sites, $k_f=10^8$ M^{-1} s^{-1}, $k_r=0.2$ s^{-1}).

tion of polymer concentration in the solution as well as polymer length.

The gap distributions corresponding to the equilibrium charge neutralizations of Fig. 10 are presented in Fig. 11. It can be seen that irreversible binding results in a uniform distribution of gap (overlap) sizes and that when removal occurs the number of gaps decreases as the gaps increase in size; that is, larger overlaps are less frequent, a similar result to that presented in Fig. 5, where the incluion of removal leads to a more pronounced, size-dependent gap distribution.

Since longer polymers have more charge than their shorter counterparts, their binding rate constant may differ from those of shorter polymers. Considering only the solid and the dashed lines in Fig. 9, the initial concentration of the polymers (L_0) is set to be the same in both cases. As a result there is much greater unneutralized charge of free polymers when $x=20$ than when $x=5$. The free polymer concentration

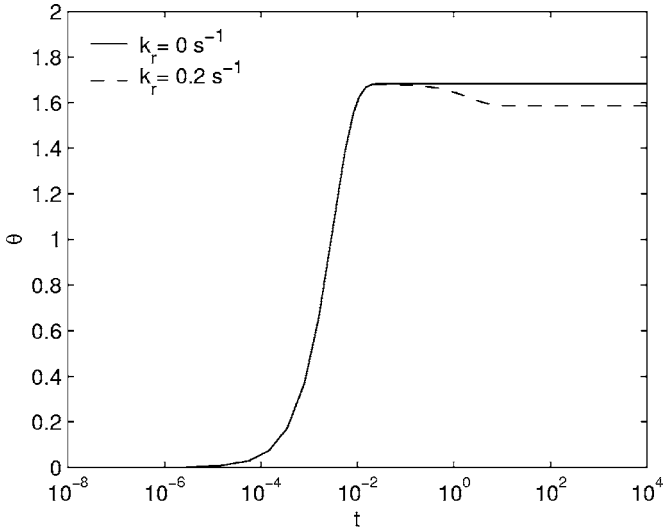

FIG. 10. Effect of removal on charge neutralization. Parameter values $L_0=10^{-6}$ M, $A_0=5\times10^{-9}$ M, $P_0=200$ sites, $x=5$ sites, $k_f=10^8$ M^{-1} s^{-1}.

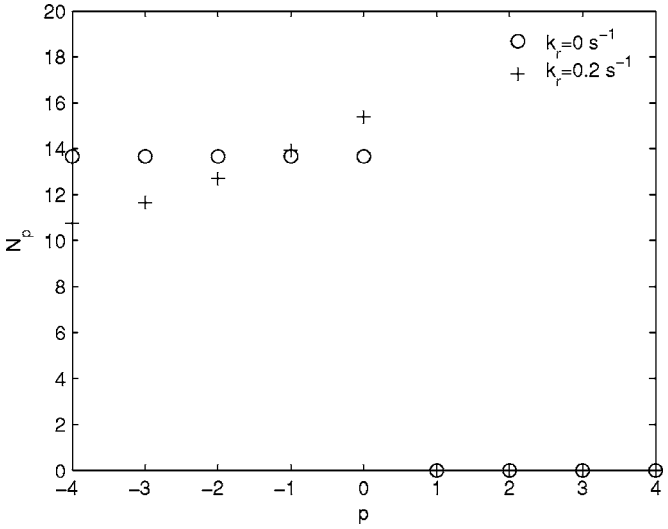

FIG. 11. Effect of removal on steady-state gap distribution ($L_0=10^{-6}$ M, $A_0=5\times10^{-9}$ M, $P_0=200$ sites, $x=5$ sites, $k_f=10^8$ M^{-1} s^{-1}).

in the solution is decreased every time one of the polymers binds to the DNA. Fewer polymers are required to cover the DNA surface if they are longer and therefore the reduction of polymer concentration in solution from $t=0$ to equilibrium will be greater in the case of shorter polymers. The effects should be even more noticeable when the initial concentration of free polymers is small.

IV. EFFECT OF MOTION ON BINDING WITHOUT OVERLAPS

A. Modeling motion

In this section we consider the case where polymers move along the plasmid; no polymers can adhere, or be removed from the plasmid and overlapped binding cannot occur. This corresponds to Eq. (6) with $F_p=0=U_p$ and $V_p\neq0$. We also assume that the initial distribution of gaps is given by $N_p(0)$. We assume that a polymer molecule can move only if it has a nonzero gap to one side of it, and that polymer motion occurs in unit steps. Figure 12 illustrates the effect of pos-

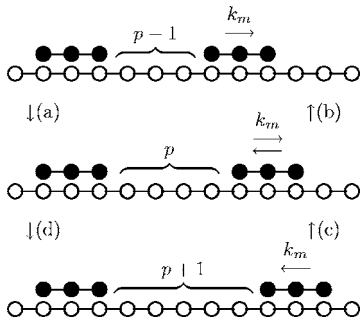

FIG. 12. Series of sketches illustrating how polymer movement can lead to the formation and destruction of a gap of length p. The processes labeled (a), (b), (c), and (d) are modeled by formulas (22a–22d), respectively.

sible motions on a gap of length p.

The effects that polymer movement, as depicted in Fig. 12, has on gap distribution are shown below

$$V_p^{f-} = k_m \underbrace{N_{p-1}\left(1 - \frac{N_0}{M_0}\right)}_{\substack{\text{gap of size} \\ p-1 \text{ grows}}}, \tag{22a}$$

$$V_p^{r-} = k_m \underbrace{N_p}_{\substack{\text{gap of size} \\ p \text{ shrinks}}}, \tag{22b}$$

$$V_p^{f+} = k_m \underbrace{N_{p+1}}_{\substack{\text{gap of size} \\ p+1 \text{ shrinks}}}, \tag{22c}$$

$$V_p^{r+} = k_m \underbrace{N_p\left(1 - \frac{N_0}{M_0}\right)}_{\substack{\text{gap of size} \\ p \text{ grows}}}, \tag{22d}$$

where k_m is the rate of polymer motion along the DNA. Superscripts + and − refer to transformations between the gap of the length p and larger and smaller gaps, respectively. As before, superscripts f and r refer to gap formation and removal, respectively. Gaps can grow only if there is a nonzero gap on the other side of the polymer, allowing the polymer to move, hence the factor $(1-N_0/M_0)$ in Eqs. (22a) and (22d), N_0/M_0 being the probability of any given gap having size zero. Using Eq. (22) to construct gap distribution kinetics equations due to polymer motion, and combining with the effects of adhesion, removal modeled by Eq. (18), we obtain

$$\frac{dN_p}{dt} = -F_p^r + U_p^f \quad (P_0 - x + 1 \le p \le P_0), \tag{23a}$$

$$\frac{dN_{P_0-x}}{dt} = F_{P_0-x}^f - F_{P_0-x}^r + U_{P_0-x}^f - U_{P_0-x}^r + V_{P_0-x}^{f-} - V_{P_0-x}^{r-}, \tag{23b}$$

$$\frac{dN_p}{dt} = F_p^f - F_p^r + U_p^f - U_p^r + V_p^{f+} + V_p^{f-} - V_p^{r+} - V_p^{r-} \quad (x \le p \le P_0 - x - 1), \tag{23c}$$

$$\frac{dN_p}{dt} = F_p^f - U_p^r + V_p^{f+} + V_p^{f-} - V_p^{r+} - V_p^{r-} \quad (1 \le p \le x - 1), \tag{23d}$$

$$\frac{dN_0}{dt} = F_0^f - U_0^r + V_0^{f+} - V_0^{r+}. \tag{23e}$$

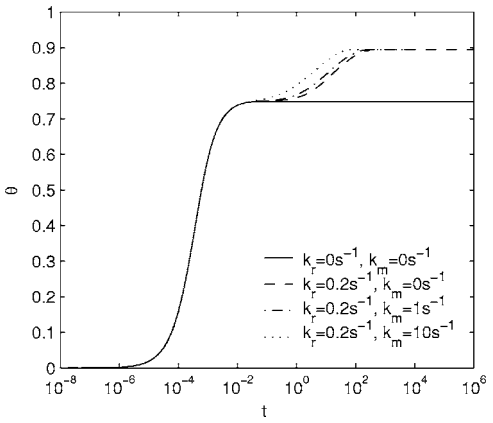

FIG. 13. Effect of polymer motion on the kinetics of charge neutralization θ. Parameter values: $L_0=10^{-6}$ M, $A_0=2\times10^{-9}$ M, $P_0=500$ sites, $x=20$ sites, $k_f=10^8$ M^{-1} s^{-1}.

B. Results for the system including adhesion, removal, and motion

The evolution of the gap distributions $N_p(t)$ was calculated by solving equations (23) numerically using a special routine for stiff systems (the subroutine D02NBF of the NAG Mark 18 FORTRAN library). The charge neutralization is calculated from $\theta=x(M_0-1)/P_0$, where M_0 is the total number of gaps.

The kinetics of charge neutralization for systems with different rates of polymer motion are displayed in Fig. 13. Numerical simulations again show that the equilibrium charge neutralization for systems with polymer removal, and with or without polymer motion are identical; the difference is that the equilibrium state is reached faster when motion is present. The equilibrium charge neutralization for systems with motion and no removal is the same as that for the systems with removal and no motion.

The equilibrium gap distributions corresponding to the charge neutralization curves shown in Fig. 13 are plotted in Fig. 14. They show that when binding is reversible and/or when motion is included, the equilibrium distribution is identical.

Figure 15 illustrates a situation when polymers cannot leave the DNA after they bind but can move along the DNA. The values of θ for reversible and irreversible binding with motion initially coincide. Irreversible binding (corresponding to dash-dotted line in Fig. 15) approaches complete charge neutralization ($\theta=1$) for large times. Such behavior is expected for any binding rate and any length of polymer since polymers simply fill all the gaps large enough to accommodate them; random polymer motion will eventually result in gaps coalescing to gaps large enough to accept further polymers until the entire DNA plasmid has been neutralized.

C. Fast motion asymptotics

An equation for charge neutralization for cases in which polymers move along the DNA molecule at much greater rates than those at which either binding or removal occur on DNA of infinite length was derived by Epstein in Ref. [5]. In

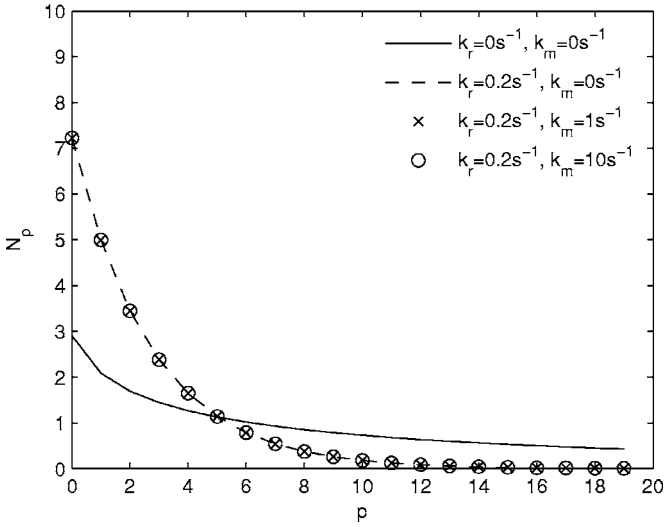

FIG. 14. Effect of polymer motion on equilibrium gap distribution N_p. Parameter values: $L_0=10^{-6}$ M, $A_0=2\times10^{-9}$ M, $P_0=500$ sites, $x=20$ sites, $k_f=10^8$ M^{-1} s^{-1}.

this section we use equations (23) to determine the charge neutralization kinetics for this case and, in so doing, confirm Epstein's results.

In the later stages of the process, when motion becomes important, only the distribution of short gaps is relevant since the large gaps will have completely disappeared. Over short time scales, no adhesion or removal occurs, and the kinetics are governed by motion. Thus, setting $F_p=U_p=0$ in Eq. (23), we have the equation for the gap distribution on the DNA plasmid in the limit of $P_0\to\infty$ is

$$\frac{1}{k_m}\frac{dN_0}{dt}=N_1-\left(1-\frac{N_0}{M_0}\right)N_0, \tag{24a}$$

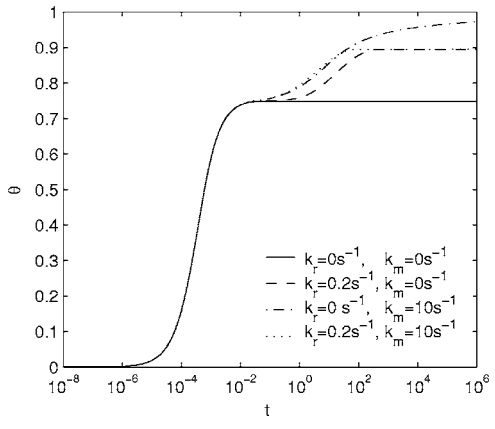

FIG. 15. Combined effects of polymer motion and removal on the kinetics of charge neutralization. Parameter values: $L_0=10^{-6}$ M, $A_0=2\times10^{-9}$ M, $P_0=500$ sites, $x=20$ sites, $k_f=10^8$ M^{-1} s^{-1}.

$$\frac{1}{k_m}\frac{dN_p}{dt}=N_{p+1}-\left(1-\frac{N_0}{M_0}\right)N_p-N_p+\left(1-\frac{N_0}{M_0}\right)N_{p-1}\ (p\geq1), \tag{24b}$$

where $M_0=\Sigma_{p=0}^{\infty}N_p$ and hence $\frac{d}{dt}M_0$ is an order of magnitude smaller than M_0.

At equilibrium Eq. (24a) implies

$$N_1=N_0\left(1-\frac{N_0}{M_0}\right). \tag{25}$$

When $\frac{d}{dt}N_p=0$, equations (24b) form a system of linear, constant coefficient, recurrence relations whose solution is given by

$$N_p(t)=N_0\left(1-\frac{N_0}{M_0}\right)^p, \tag{26}$$

for any choice of the parameters N_0, M_0. For a given system, M_0 should be constant over the time scale considered in Eq. (24b). This suggests that there is a two-parameter family of solutions to Eq. (24a), parametrized by N_0 and M_0, N_0 being the number of gaps of zero length and M_0 being the total number of gaps (of any size).

Assuming Eq. (26) holds for $0\leq p\leq P_0$ and $P_0\gg1$, we have

$$M_1=\frac{M_0}{N_0}(M_0-N_0). \tag{27}$$

An expression relating the number of gaps of size zero to M_0 is found by applying the identity $P_0-M_1=x(M_0-1)$ to Eq. (27). This gives

$$N_0=\frac{M_0^2}{P_0+x+(1-x)M_0}. \tag{28}$$

At any particular time we expect the shape of the distribution $N_p(t)$ to be given by Eq. (26) with Eq. (28) and $0<M_0<1+P_0/x$.

Over large times $M_0(t)$ will vary as polymers slowly adhere to the DNA or are removed from it. We substitute for N_0 from Eq. (28) into Eq. (26) to get the approximate distribution for all gap sizes

$$N_p(t)=\frac{M_0^2}{P_0+x+(1-x)M_0}\left(\frac{P_0+x-xM_0}{P_0+x+(1-x)M_0}\right)^p, \tag{29}$$

where the only time dependence is via $M_0(t)$ which we determine below. Since we expect $N_p=0$ for $p\gg x$, this will be a good approximation only in the later stages of the polymer adhesion process, where N_p is small for $p\geq x$.

We now derive an evolution equation for M_0 that is valid at large times when polymer adhesion and removal occurs. From Eq. (23) we obtain the ODE

$$\frac{dM_0}{dt}=\sum_{p=0}^{P_0-x}\left(K_f(p+1)N_{p+x}-K_rN_p\sum_{q=0}^{P_0-p-x}N_q\right). \tag{30}$$

To close the system, we substitute from Eq. (29) into Eq. (30), write $K_r=k_r/M_0$ and

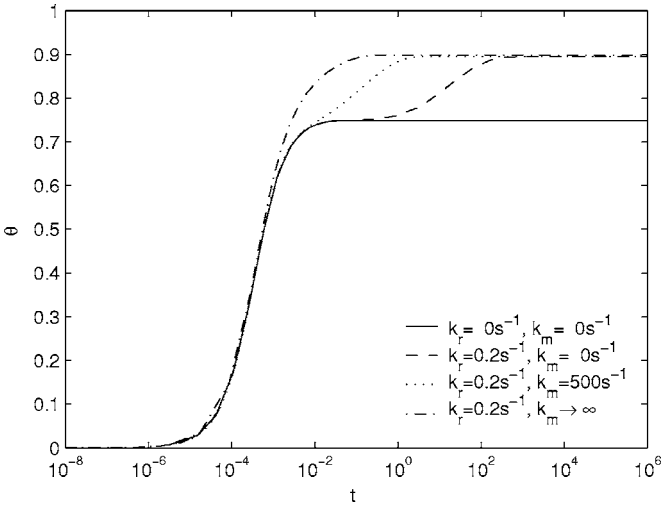

FIG. 16. Asymptotic solution of charge neutralization kinetics ($L_0=10^{-6}$ M, $A_0=2\times10^{-9}$ M, $P_0=500$ sites, $x=20$ sites, $k_f=10^8$ M^{-1} s^{-1}).

$$K_f = k_f L(t) = k_f[L_0 - A_0(M_0 - 1)],$$

and set the upper limits in Eq. (30) to infinity. In this way, we obtain

$$\frac{dM_0}{dt} = \frac{k_f[L_0 - A_0(M_0-1)][P_0 - x(M_0-1)]^x}{[P_0 - x(M_0-1) + M_0]^{x-1}} - k_r M_0. \tag{31}$$

Using $\theta = x(M_0-1)/P_0$, we rewrite this as an evolution equation for the charge neutralization which, on taking the limit $P_0 \to \infty$, yields

$$\frac{d\theta}{dt} = \frac{k_f x[L_0 - A_0(M_0-1)](1-\theta)^x}{\left[1 - \left(\frac{x-1}{x}\right)\theta\right]^{x-1}} - k_r\theta. \tag{32}$$

Epstein's derivation is based on the McGhee–von Hippel isotherm [25]. In Ref. [5], Epstein uses θ to denote the quantity $(M_0-1)/P_0$ so to convert to our charge neutralization variable $\theta = x(M_0-1)/P_0$ we rescale multiply Epstein's θ by x. Equation (18) of Ref. [5] is thus transformed into Eq. (32) above.

Equation (31) is applicable to the binding of polymers that have a high rate of movement along the DNA molecule. The steady state solution of Eq. (31) also applies to the polymers that do not move along the DNA ($k_m=0$) but are removable ($k_r>0$). Numerical solutions of Eq. (31) are plotted in Fig. 16. As expected, the steady-state charge neutralization is the same regardless of whether the polymers move. The time taken to approach that state is considerably reduced when the polymers move. All curves display identical behavior on the faster time scale when the binding process dominates.

We now use Eq. (32) to calculate two further quantities: first, the rate at which the charge neutralization approaches unity in the case where there is motion and no removal, and secondly the equilibrium charge neutralization when the removal rate is small.

1. Equilibrium charge neutralization in the case of small removal rates

We consider the case where the polymers are long, and the DNA plasmid is extremely long, so that it can accommodate many polymers. Thus we use the scalings $x=1/\epsilon$ and $P_0=y/\epsilon^2$ with $\epsilon \ll 1$. This implies that, to leading order, $M_0=\theta/\epsilon$, and that Eq. (31) simplifies to

$$\frac{d\theta}{dt} = -k_r\theta + \frac{k_f}{\epsilon^2}(L_1 - A_0\theta y)(1-\theta)\exp\left(\frac{-\theta}{1-\theta}\right), \tag{33}$$

where $A_0=O(1)$ and $L_0 \approx L_1/\epsilon$ with $L_1=O(1)$.

As shown above, if there is motion with no removal, the equilibrium charge neutralization is unity. However, in the case of motion with *reversible* binding, the equilibrium value of θ is below unity. To obtain an asymptotic expression for the equilibrium value when k_r is small we write $\theta=1-\delta$ with $\delta \ll 1$. From Eq. (33) we find that at equilibrium

$$\frac{1}{\delta}e^{1/\delta} = \frac{k_f}{k_r\epsilon^2}(L_1 - A_0 y) =: q, \tag{34}$$

and $1/\delta = W(q)$, where W is Lambert's function [26] which has the property that $W(q) \sim \ln q$ for $q \gg 1$. Thus for systems with a small removal rate the equilibrium charge neutralization is given by

$$\theta \sim 1 - \frac{1}{\ln[k_f(L_1 - A_0 y)/k_r\epsilon^2]} \tag{35}$$

or, reintroducing the scales $x=1/\epsilon$ and $P_0=y/\epsilon^2$,

$$\theta \sim 1 - \frac{1}{\ln[k_f(L_0 x - A_0 P_0)/k_r]}. \tag{36}$$

The accuracy of this asymptotic solution is investigated in the next section.

2. Large-time solution for the case of motion with no removal

If there is polymer motion, but no removal then the charge neutralization approaches exactly unity in the large-time limit. To analyze the large-time solution in this case, we return to Eq. (33) noting that $k_r=0$. We expect $\theta \to 1$ as $t \to \infty$. The large-scale asymptotics can be derived by introducing $\psi = 1-\theta \ll 1$ for which

$$\epsilon^2\frac{d\psi}{dt} = -k_f(L_1 - A_0 y)\psi e^{-1/\psi}. \tag{37}$$

Hence we find that $\theta(t) \sim 1 - 1/\ln(t)$ as $t \to \infty$, which gives the extremely slow convergence seen in the top curve of Fig. 15.

D. Charge neutralization as a function of removal rate

We now study the effect of varying the ratio of binding to removal rates on the equilibrium charge neutralization. Steady-state solutions for reversible binding with different

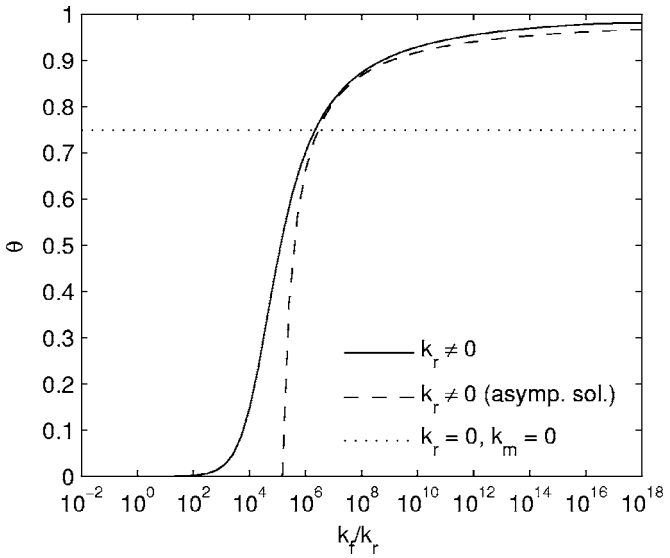

FIG. 17. Steady-state charge neutralization calculated from numerical solution of Eq. (31) (solid line), asymptotic solution (36) (dashed line), and the recurrence relation [1] (dotted line). Parameter values: $L_0=10^{-6}$ M, $A_0=2\times10^{-9}$ M, $P_0=500$ sites, $x=20$ sites, $k_f=10^8$ M^{-1} s^{-1}.

values of k_f/k_r are compared to irreversible binding solutions in Fig. 17.

The solid line in Fig. 17 represents the steady-state solution of Eq. (31) for various values of k_f/k_r. The dotted line corresponds to the steady-state of the irreversible binding system where it is assumed that polymers cannot leave ($k_r=0$) or move along ($k_m=0$) the DNA once attached. The two curves intersect when $k_f/k_r=\kappa_0=2.09\times10^6$ M^{-1}. The dashed line in Fig. 17 corresponds to asymptotic solution (36). We observe good agreement for $k_f/k_r>10^6$.

E. Kinetics of high removal-rate reactions

We now examine the effects of varying the removal and movement rates on charge neutralization. Figure 18 shows the kinetics of charge neutralization for irreversible binding (circles) together with three pairs of curves. In each pair, one curve corresponds to no motion and the other to extremely rapid motion. We define $\kappa_0=k_f/k_r$ for the value of this ratio which gives an equilibrium charge neutralization equal to that which occurs in the pure adhesion case ($k_r=0=k_m$); from the above subsection we note that $\kappa_0=2.09\times10^6$ M^{-1}. The definition of κ implies $k_f=k_r\kappa_0\kappa$ so that large values of κ represent adhesion-dominated systems while $\kappa<1$ indicates that removal plays the dominant role. We specify a removal rate through κ such that $k_r=k_f/\kappa_0\kappa$, thus $\kappa=10$ corresponds to a low removal rate, and $\kappa=0.1$, a high removal rate.

In Fig. 18, the solid line with bars across it corresponds to binding when polymers are assumed to move rapidly along the DNA plasmid ($k_m\to\infty$, $\kappa=1$). The unmarked solid line corresponds to the reversible process when polymers do not move along the DNA plasmid ($k_m=0$, $\kappa=1$). Both cases with $\kappa=1$ yield results that are very close to irreversible binding but high movement rates leads to slightly higher charge neutralization than when $k_m=0$.

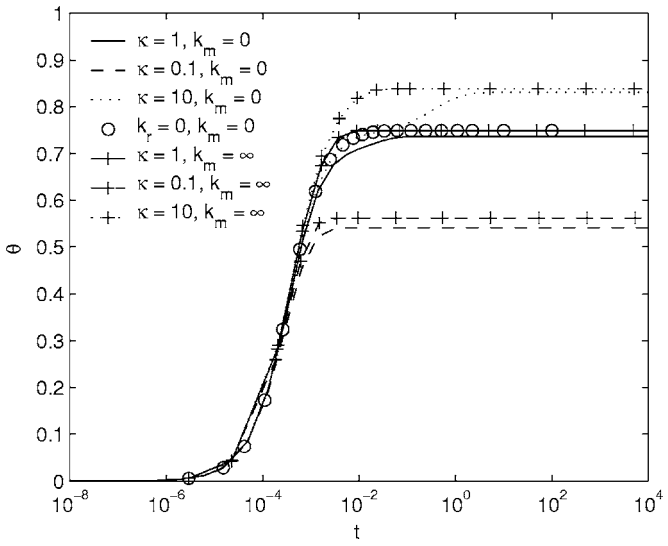

FIG. 18. Kinetics of charge neutralization for various values of the removal rate [$L_0=10^{-6}$ M, $A_0=2\times10^{-9}$ M, $P_0=500$ sites, $x=20$ sites, $\kappa=k_f/(k_r\kappa_0)$, $\kappa_0=2.09\times10^6$ M^{-1}].

When the removal rate is high ($\kappa=0.1$) the charge neutralization is low ($\theta\approx0.55$) and again motion causes a slight increase in θ. The same qualitative behavior is observed when the removal rate is low ($\kappa=10$) except that the charge neutralization is much higher ($\theta\approx0.83$). The results presented in Fig. 18 suggest that using Eq. (32) to determine the steady state charge neutralization may underestimate the correct solution when the removal rate is relatively low.

V. MODELING MOTION WITH OVERLAPS

A. Pure motion

In this section we consider the case where a finite number of polymer molecules are attached to the DNA. The polymers can move along the plasmid, but no further polymer can adhere, and none can be removed.

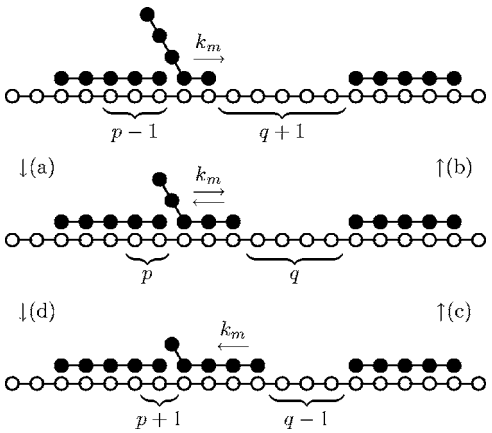

FIG. 19. Illustration of p-gap formation and destruction due to polymer motion; in this case $p<0$ so the "gap" is actually an overlap. The processes (a)–(d) are modeled by formulas (38a)–(38d), respectively.

We assume that the initial distribution of gaps is given by $N_p(0)$ and since overlaps are permitted, $-(x-1) \leq p \leq P_0$. We wish to determine how this distribution evolves due to the allowed motion of adhered polymer molecules. We suppose that a polymer molecule will always move unless it has reached maximum possible overlap $p=-x+1$ on one side, and that each motion corresponds to the motion of a polymer over one lattice site. Figure 19 illustrates the range of effects that polymer movement can have on gaps of length p.

The effects that polymer movements (a)–(d) displayed in Fig. 19 have on the gap distribution are shown below

$$V_p^{f-} = k_m \underbrace{\left(1 - \frac{N_{1-x}}{M_0}\right) N_{p-1}}_{\substack{\text{gap of size} \\ p-1 \text{ grows}}}, \tag{38a}$$

$$V_p^{r-} = k_m \underbrace{N_p}_{\substack{\text{gap of size} \\ p \text{ shrinks}}}, \tag{38b}$$

$$V_p^{f+} = k_m \underbrace{N_{p+1}}_{\substack{\text{gap of size} \\ p+1 \text{ shrinks}}}, \tag{38c}$$

$$V_p^{r+} = k_m \underbrace{N_p \left(1 - \frac{N_{1-x}}{M_0}\right)}_{\substack{\text{gap of size} \\ p \text{ grows}}} \tag{38d}$$

As before, superscripts f and r refer to gap formation and removal, respectively, and k_m is the rate of polymer motion along the DNA. The additional superscripts $\pm$ refer to transitions between gaps of length p and $p \pm 1$, respectively.

Using Eq. (38) to construct equations for the evolution of the gap distribution, combining with the effects of adhesion, and removal modeled by Eq. (21), we obtain

$$\frac{dN_{P_0}}{dt} = -F_{P_0}^r + U_{P_0}^f, \tag{39a}$$

$$\frac{dN_{P_0-1}}{dt} = F_{P_0-1}^f - F_{P_0-1}^r + U_{P_0-1}^f - U_{P_0-1}^r + V_{P_0-1}^{f-} - V_{P_0-1}^{r-}, \tag{39b}$$

$$\frac{dN_p}{dt} = F_p^f - F_p^r + U_p^f - U_p^r + V_p^{f+} + V_p^{f-} - V_p^{r+} - V_p^{r-} \quad (1 \leq p \leq P_0 - 2), \tag{39c}$$

$$\frac{dN_p}{dt} = F_p^{f-} + U_p^f - U_p^r + V_p^{f+} + V_p^{f-} - V_p^{r+} - V_p^{r-} \quad (2 - x \leq p \leq 0), \tag{39d}$$

$$\frac{dN_{1-x}}{dt} = F_{1-x}^{f-} - U_{1-x}^r + V_{1-x}^{f+} - V_{1-x}^{r+}. \tag{39e}$$

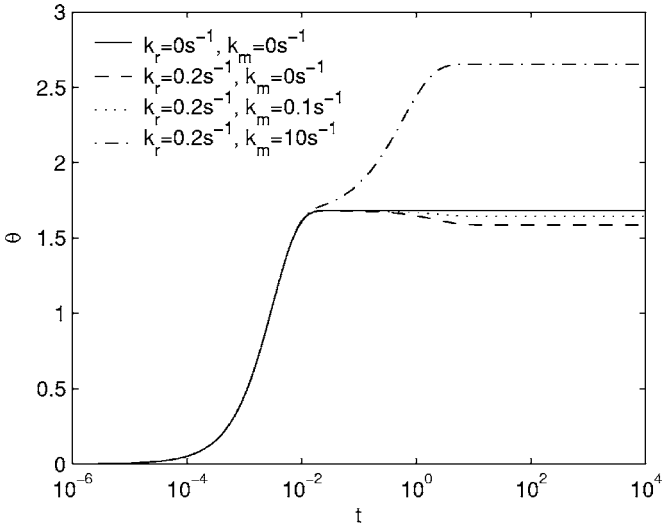

FIG. 20. Effect of polymer motion on kinetics of charge neutralization when overlaps are permitted, log scale in time ($L_0 = 10^{-6}$ M, $A_0 = 5 \times 10^{-9}$ M, $P_0 = 200$ sites, $x = 5$ sites, $k_f = 10^8$ M^{-1} s^{-1}).

B. Numerical solution for adhesion, removal, and motion

As before, the evolution of the gap distributions $N_p(t)$ was calculated by solving Eq. (39) numerically using the subroutine D02NBF from the NAG Mark 18 FORTRAN library. The charge neutralization was calculated from $\theta = x(M_0 - 1)/P_0$, where M_0 is the total number of gaps.

In Fig. 20 we compare charge neutralization for polymer binding with and without motion. Recall that with overlapped binding, polymer removal leads to a reduction in charge neutralization over larger time scales. Even a relatively slow rate of movement results in a large increase in charge neutralization (dotted line in Fig. 20) compared to that without movement (dashed line in Fig. 20). Increasing the rate of movement further results in a further increase of charge neutralization (dash-dot line in Fig. 20).

When systems allowing motion with overlaps (Fig. 20) are compared with systems allowing motion without overlaps (Fig. 13), it is clear that allowing overlaps leads to a further large increase in charge neutralization. In the case of binding without overlaps movement merely resulted in a faster approach to the reversible binding equilibrium.

Further information about the system can be obtained by studying the gap distribution (see Fig. 21). The data marked by $\times$'s in Fig. 21 correspond to the largest movement rate, and shows a large number of overlaps of the largest possible size. Rearrangements which increase the size of overlaps when the DNA plasmid is already fully covered lead to this scenario where very large charge neutralizations observed, as shown in Fig. 20, and are almost certainly unphysical. This is due to an oversimplified model of polymer motion; a more accurate model of polymer motion would take account of a charge-charge interactions and hence favor motion which led to a reduction in overlap size.

The charge neutralization process can be limited by preventing motions that increase the number or size of existing overlaps. Removing all movement terms that lead to the for-

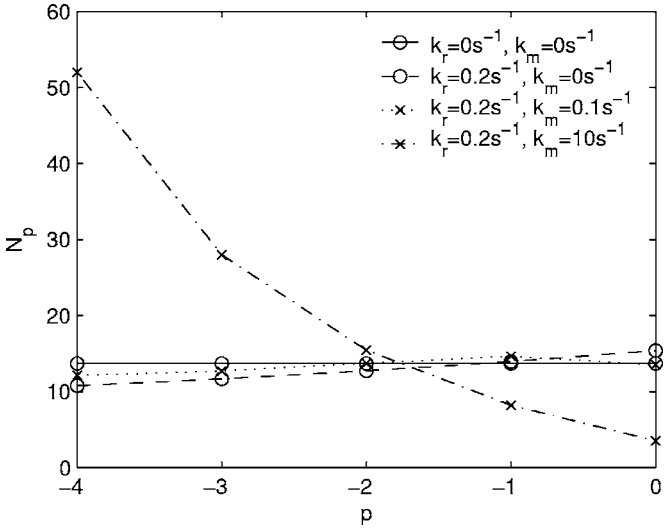

FIG. 21. Effect of polymer motion on equilibrium gap distribution ($L_0=10^{-6}$ M, $A_0=5\times10^{-9}$ M, $P_0=200$ sites, $x=5$ sites, $k_f=10^8$ M^{-1} s^{-1}).

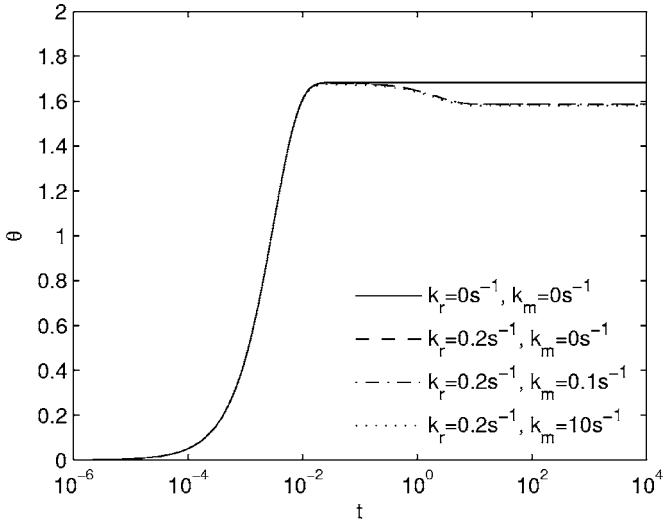

FIG. 22. Effect of limited polymer motion [Eq. (40)] on the kinetics of charge neutralization, log scale in time ($L_0=10^{-6}$ M, $A_0=5\times10^{-9}$ M, $P_0=200$ sites, $x=5$ sites, $k_f=10^8$ M^{-1} s^{-1}).

mation of overlaps from equations (39) gives the more physically realistic equations

$$\frac{dN_{P_0}}{dt} = 0, \tag{40a}$$

$$\frac{1}{k_m}\frac{dN_{P_0-1}}{dt} = -N_{P_0-1}, \tag{40b}$$

$$\frac{1}{k_m}\frac{dN_p}{dt} = N_{p+1} - N_p \quad (P_0 - x + 1 \le p \le P_0 - 2),$$

$$\frac{1}{k_m}\frac{dN_{P_0-x}}{dt} = N_{P_0-x+1} - N_{P_0-x} + N_{P_0-x-1}S, \tag{40c}$$

$$\frac{1}{k_m}\frac{dN_p}{dt} = -N_pS + N_{p+1} - N_p + N_{p-1}S \quad (1 \le p \le P_0 - x - 1), \tag{40d}$$

$$\frac{1}{k_m}\frac{dN_0}{dt} = -N_0S + N_1 + N_{-1}S, \tag{40e}$$

$$\frac{1}{k_m}\frac{dN_p}{dt} = -N_pS + N_{p-1}S \quad (2 - x \le p \le -1), \tag{40f}$$

$$\frac{1}{k_m}\frac{dN_{1-x}}{dt} = -N_{1-x}S, \tag{40g}$$

where $S=\frac{1}{M_0}\Sigma_{q=1}^{P_0}N_q$ is the proportion of gaps which are positive in length and k_m is the rate of motion.

Charge neutralization of the system with motion limited to reducing overlaps is shown in Fig. 22. Polymer motion modeled by Eq. (40) neither increases the charge (as it did in Fig. 20), nor results in the same charge neutralization as irreversible binding without motion (Fig. 13 in Sec. IV B). The graph corresponding to polymers with motion rate $k_m=0.1$ s^{-1} in Fig. 22 shows that motion results in a slight decrease in the charge neutralization θ with the line corresponding to $k_m=10$ s^{-1} confirming the result with charge neutralization decreasing a little further. The kinetics of charge neutralization in the system with modified motion still occur on the same time scales: with binding on a time scale of 10^{-3}–10^{-2}, and rearrangements leading to reduction in θ over $t\sim10^{-1}$–10^{+1}.

VI. DISCUSSION

We have developed a deterministic model of the kinetics of gap distributions occurring when polymers bind reversibly, with or without overlaps, to DNA. We have verified that the numerical simulations agree with equivalent Monte Carlo simulations. The results confirmed that removal generally increases the charge neutralization when polymers do not overlap and decreases it when they do. We have also determined the distribution of gaps or overlaps at equilibrium. In the nonoverlapping case, introducing reversible adhesion accentuates the size dependence of gap sizes, making smaller gaps more common and larger gaps less common than in the case of irreversible adhesion (Fig. 6). When overlaps are permitted, irreversible binding produces a distribution of overlaps which is independent of size, whereas when binding is reversible small overlaps are more frequent and large gaps less common (Fig. 11).

Reducing the free polymer concentration had a less pronounced effect on charge neutralization in the case of overlapping than in the nonoverlapping case. The decrease in charge neutralization observed in nonoverlapped binding with lower concentration of polymers in the solution was not observed when overlaps were allowed.

We have also extended our deterministic model to allow for polymer motion along the DNA plasmid. Numerical so-

lutions of the nonoverlapping process are in good agreement with Monte Carlo simulations and suggest that motion decreases the time taken to reach the equilibrium charge neutralization.

Polymer motion in the overlapped system can have a dramatic effect on the equilibrium charge neutralization. Our initial model of polymer motion allows polymers to move towards and over each other until they form the maximum possible overlap. This leads to a greatly increased equilibrium charge neutralization, through an effect which we believe is unphysical. Although other authors have commented on the possibility of such large charge inversions [27], in many systems we believe there will be an upper limit to observed charge inversions, as noted by Tanaka and Grosberg [28]. Hence, we have proposed a modified model in which polymer motion can only decrease overlap size. The corresponding equilibrium charge neutralization is decreased.

We have considered one asymptotic domain in more detail, namely the case of long polymers (of length $x=1/\varepsilon$ with $\varepsilon \ll 1$) and very long DNA plasmids [of length $P_0 = \mathcal{O}(1/\varepsilon^2)$]. In the case of reversible binding without overlaps we have determined numerically how the ratio (k_f/k_r) influences the equilibrium charge neutralization, in particular we have found an asymptotic approximation which is valid when k_f/k_r is large. Our model is based on the theory of random sequential adsorption (RSA), an approach which has been widely used previously to analyze the geometric effects of binding and blockage of binding of polymers to a DNA plasmid. The aspects we have introduced here are the combination of reversible adhesion and motion of the polymers along the plasmid. In Sec. IV C we have used an asymptotic analysis to show that the system exhibits extremely slow kinetics in its approach to equilibrium.

Future work could be directed at deriving more refined formulas for the adhesion and removal rates' and their dependence on electrostatic DNA-polymer interactions. The resulting models would then be more consistent with the electrostatic and thermodynamic models of Ref. [29]. In a future paper we address DNA-polymer interactions in which the polymers have a polydisperse distribution of lengths [31,32].

In summary, our analysis of the kinetics of charge neutralization reveals four qualitatively different types of behavior (see Fig. 23). The simplest model of irreversible binding without overlaps predicts a one-step monotonic increase in the charge neutralization (solid line in Fig. 23). This is always insufficient to cause DNA condensation regardless of the length of the polymer as it is below the 90% needed to condense DNA (Wilson and Bloomfield [30]). When binding is reversible and without overlaps (dashed line) the dynamics exhibit a two-step monotonic increase to a higher equilibrium charge neutralization. The counterintuitive result that including polymer removal causes an increase in charge neutralization is due to the fact that removal creates gaps large enough for a greater number of polymers to bind to the DNA. Irreversible binding with overlaps (dotted line in Fig. 23) exhibits the same one-step monotonic increase as irreversible binding without overlaps but leads to a much higher charge neutralization ($\theta > 1$). The approach to the equilibrium charge neutralization is nonmonotonic when there is reversible binding with overlaps. These four types of behavior discussed above could be matched to experimental data to predict which of the mechanisms present in our family of models of polymer binding are relevant for a particular system.

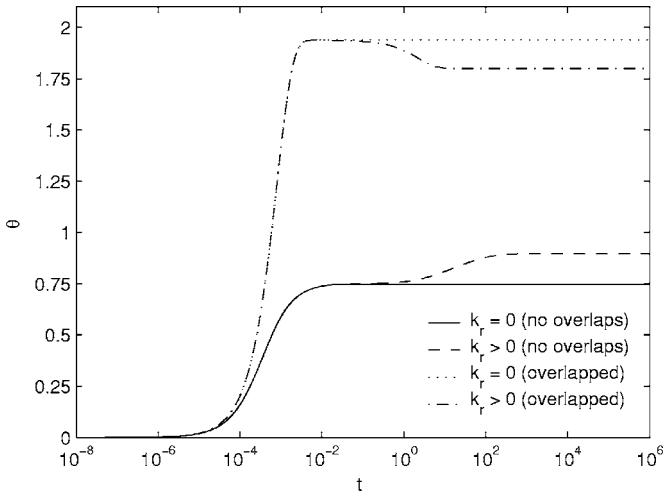

FIG. 23. Illustration of the main qualitative features of the charge neutralization kinetics of various models of polymer binding.

ACKNOWLEDGMENTS

We are grateful to Snow Stolnik and Clive Roberts for useful discussions regarding modeling and parameter values. E.M. was sponsored by the UK BBSRC.

[1] E. Maltsev, J. A. D. Wattis, and H. M. Byrne, Phys. Rev. E **74**, 011904 (2006); URL http://www.vjbio.org, 2006.
[2] A. Rényi, Acta Math. Acad. Sci. Hung. **3**, 109 (1958).
[3] B. Bonnier, D. Boyer, and P. Viot, J. Phys. A **27**, 3671 (1994).
[4] I. R. Epstein, Biopolymers **18**, 765 (1979).
[5] I. R. Epstein, Biopolymers **18**, 2037 (1979).
[6] D. Porschke, Biochemistry **23**, 4821 (1984).
[7] A. U. Bielinska, C. Chen, J. Johnson, and J. R. Baker Jr., Bioconjugate Chem. **10**, 843 (1999).
[8] J. Talbot, G. Tarjus, P. R. van Tassel, and P. Viot, Colloids Surf., A **165**, 287 (2000).
[9] E. Ben-Naim and P. L. Krapivsky, J. Phys. A **27**, 3575 (1994).
[10] P. L. Krapivsky and E. Ben-Naim, J. Chem. Phys. **100**, 6778 (1994).
[11] L. R. Brewer, M. Corzett, and R. Balhorn, Science **286**, 120 (1999).
[12] L. R. Brewer, M. Corzett, E. Y. Lau, and R. Balhorn, J. Biol. Chem. **278**, 42403 (2003).

[13] M. A. Lever, J. P. H. Th'ng, X. Sun, and M. J. Hendzel, Nature (London) **408**, 873 (2000).
[14] G. Tarjus, P. Schaaf, and J. Talbot, J. Chem. Phys. **93**, 8352 (1990).
[15] J. W. Evans, in *Nonequilibrium Statistical Mechanics in One Dimension*, edited by V. Privman (Cambridge University Press, Cambridge, 1997).
[16] M. Barma, in *Nonequilibrium Statistical Mechanics in One Dimension* [15].
[17] P. R. van Tassel, G. Tarjus, and P. Viot, J. Chem. Phys. **106**, 761 (1997).
[18] V. B. Teif, Biophys. J. **89**, 2574 (2005).
[19] A. Y. Grosberg, T. T. Nguyen, and B. I. Shklovskii, Rev. Mod. Phys. **74**, 329 (2002).
[20] G. S. Manning, Q. Rev. Biophys. **2**, 179 (1979).
[21] I. Rouzina and V. A. Bloomfield, J. Phys. Chem. **100**, 4305 (1996).
[22] E. R. Cohen and H. Reiss, J. Chem. Phys. **38**, 680 (1962).
[23] B. J. Rackstraw, A. L. Martin, S. Stolnik, C. J. Roberts, M. C. Garnett, M. C. Davies, and S. J. B. Tendler, Langmuir **17**, 3185 (2001).
[24] W. H. Press, S. A. Teukolsky, W. T. Vetterling, and B. P. Flannery, *Numerical Recipes in Fortran 90, The Art of Parallel Scientific Computing* (Cambridge University Press, Cambridge, 1996), Vol. 2.
[25] J. D. McGhee and P. H. von Hippel, J. Mol. Biol. **86**, 469 (1974).
[26] E. W. Weisstein, http://mathworld.wolfram.com/LambertW-Function.html, 2005.
[27] T. T. Nguyen, A. Y. Grosberg, and B. I. Shklovskii, Phys. Rev. Lett. **85**, 1568 (2000).
[28] M. Tanaka and A. Y. Grosberg, J. Chem. Phys. **115**, 567 (2001).
[29] I. Rouzina and V. A. Bloomfield, J. Phys. Chem. **100**, 4292 (1996).
[30] R. W. Wilson and V. A. Bloomfield, Biochemistry **18**, 2192 (1979).
[31] E. Maltsev, J. A. D. Wattis, and H. M. Byrne (unpublished).
[32] E. Maltsev, Ph.D. thesis, University of Nottingham, Nottingham 2005.